

UNCLASSIFIED

Defense Technical Information Center
Compilation Part Notice

ADP012224

TITLE: Processing Effects on the Morphology of Hydrothermally Derived Nanocrystalline Lead Titanate

DISTRIBUTION: Approved for public release, distribution unlimited

This paper is part of the following report:

TITLE: Nanophase and Nanocomposite Materials IV held in Boston, Massachusetts on November 26-29, 2001

To order the complete compilation report, use: ADA401575

The component part is provided here to allow users access to individually authored sections of proceedings, annals, symposia, etc. However, the component should be considered within the context of the overall compilation report and not as a stand-alone technical report.

The following component part numbers comprise the compilation report:

ADP012174 thru ADP012259

UNCLASSIFIED

PROCESSING EFFECTS ON THE MORPHOLOGY OF HYDROTHERMALLY DERIVED NANOCRYSTALLINE LEAD TITANATE.

Zhiyuan Ye, Elliott B. Slamovich, and Alexander H. King
School of Materials Engineering, Purdue University,
West Lafayette, IN 47906, U.S.A.

ABSTRACT

Nanocrystalline lead titanate was synthesized by reacting nanocrystalline titanium oxide in aqueous solutions of potassium hydroxide and lead acetate at 200 degrees C. X-ray diffraction (XRD) and TEM studies suggest that the initial KOH concentration influenced the nucleation and growth behavior of the lead titanate nanoparticles. Powders were processed in aqueous solutions containing 0.10 M lead acetate and a Pb:Ti ratio of 1, with varying concentrations of KOH. Powders processed in 0.01 M KOH were composed of irregularly shaped particles with 50-100 nm in size, processing in 0.10 M KOH produced particles with finger-like morphology and broader particle size distribution, and processing in 1.0 M KOH resulted in anisometric plates with (001) facets, and 100-200 nm in size. XRD studies have shown systematic variations in the position and symmetry of reflections with a l component as a function of particle size. This indicates that the c/a ratio of lead titanate increases with decreasing nanoparticle size.

INTRODUCTION

Hydrothermal processing, which involves reaction of aqueous solutions or suspensions of precursor and precipitation of complex oxides at elevated temperatures and pressures, has been widely applied in producing multicomponent metal oxide ceramic powders and thin films [1]. The ABO_3 perovskites, such as barium titanate and lead titanate, have been successfully fabricated by hydrothermal technique under various conditions [2-6]. Hydrothermal synthesis of high phase purity, ultrafine, crystalline $PbTiO_3$ has been demonstrated by several groups at temperatures lower than 200 °C.[7-10] Compared to other processing methods such as solid-state reaction, sol-gel and coprecipitation, hydrothermal processing does not require going through a high temperature calcinations step, which causes particle coarsening and agglomeration [1]. Lower processing temperatures mean reduced energy budget. In the case of $PbTiO_3$, elimination of calcinations step also avoids lead volatilization [11]. Furthermore, by varying the processing parameters like temperature, pH, and the reagent concentrations, it is possible to control the size distribution and the morphology of final products [1,9].

Hydrothermal synthesis of $PbTiO_3$ has been extensively investigated experimentally and theoretically [3,4,7,10,11]. Thermodynamic calculations and experiments by Lencka and Riman [4] revealed the phase stability diagram under hydrothermal conditions. The phase stability diagram provided profound information about optimal process setup. However, the detail particle nucleation and coarsening mechanism remained unknown. Morphology studies not only were important for application, but also could provide more insight of the mechanism. Vast literatures have been devoted to the morphology [2,3,6,7,9]. High pH generally resulted in faster reaction rate and cuboidal morphology, while low pH could result in acicular or platelet morphology. In this paper, the influence of the concentration of mineralizer KOH, in turn the pH in starting suspensions on the resulting morphology will be presented. A possible mechanism of morphological evolution under different initial KOH concentration is proposed to explain the observations.

EXPERIMENTAL PROCEDURE

Hydrothermal PbTiO_3 nanoparticles were processed by mixing nanocrystalline TiO_2 (P25, Degussa, Dublin, OH) with lead acetate trihydrate ($\text{Pb}(\text{CH}_3\text{COO})_2 \cdot 3\text{H}_2\text{O}$, Aldrich, 99+% purity) at a 1:1 molar ratio, then suspended in aqueous KOH in a Teflon lined autoclave (Model No. 4748, Parr Instrument Co., Moline, IL). The KOH solution was prepared by dissolving KOH (Mallinckrodt, 85% KOH, $\approx 15\%$ H_2O) in boiling CO_2 -free deionized water. The autoclave was then placed into a preheated force-air oven, holding at 200°C for reaction under autogenous conditions. After reaction, the autoclave was force-air cooled to room temperature. The suspension was vacuum filtered, repeatedly washing with CO_2 -free deionized water. The collected powders were dried overnight at 90°C . PbTiO_3 nanoparticles were examined by X-ray diffraction (XRD) (Siemens D500 diffractometer) using $\text{CuK}\alpha$ radiation. Particle size and morphology were characterized by transmission electron microscopy (TEM) (JEOL 2000FX).

The processing parameters were varied systematically to examine effects on particle morphology. The feedstock of every run maintained a lead concentration of 0.1M with $[\text{Pb}]/[\text{Ti}] = 1.0$. KOH concentrations of 0.01M, 0.1M and 1M, with processing time from 6hrs to 12hrs to 24hrs, were investigated.

RESULTS AND DISCUSSIONS

X-ray diffraction (XRD) observations

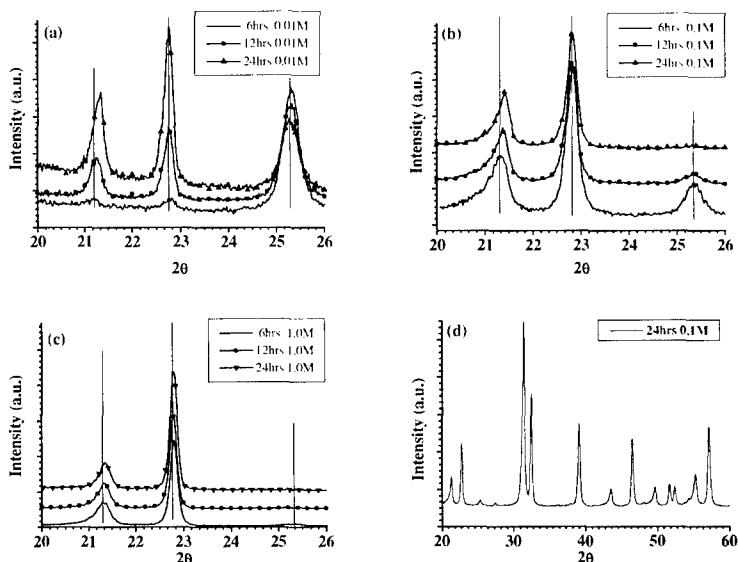


Figure 1. XRD patterns of PbTiO_3 nanoparticles processed at 200°C with $[\text{Pb}]=[\text{Ti}]=0.1\text{M}$. Initial KOH concentrations and processing time of (a),(b) and (c) are as indicated in legends. Vertical lines are guides for eyes. (001) peak ($\approx 21.4^\circ$) and (100) peak ($\approx 22.8^\circ$) of PbTiO_3 and peak for TiO_2 (anatase, $\approx 25.4^\circ$) are shown. (d) is a typical PbTiO_3 XRD pattern with 2θ from 20° to 60° .

XRD patterns of the collected powders prepared under different conditions show that the powders are composed of either pure PbTiO_3 or mixture of PbTiO_3 and unreacted TiO_2 . This indicates that, under the processing conditions, PbTiO_3 is the only reaction product, which agrees with the majority of the literature (Figure 1).

The significant changes of relative intensities between PbTiO_3 and TiO_2 in Figure 1 (a), (b) and (c) along with time reflect the progress of reaction. The initial KOH concentration, or the pH has great influence on reaction rate. At 1.0M KOH, the residual TiO_2 is not detectable via XRD within 12 hours, while it takes 24 hours for process with 0.1M KOH to reach similar point. Further experiments show that, significant amount of TiO_2 remains even after 96 hours of processing. The reaction driving force strongly depends on the pH of the starting suspension.

Figure 1. (a), (b) and (c) all show that (001) peak of PbTiO_3 systematically shift toward high 2θ as processing time increases. This indicates a decrease of lattice constant c as particle size increases (due to longer process time). This result is in line with a previous work of one of the authors.[9] The size effect on lattice of PbTiO_3 nanoparticles prepared by sol-gel technique has been studied theoretically and experimentally [12,13]. However, the reported relation was opposite to our observations [12]. This discrepancy may be attributed to slightly different stoichiometry and different morphology. Further investigation will be necessary to clarify this problem.

The (001) peaks in Figure 1. (b) show stronger asymmetric shape than those in (a) and (c). This might be also attributed to size effect on lattice constant. If this were the case, the particles from 0.1M KOH would have a broader size distribution. Our TEM observations have supported this conclusion.

Transmission electron microscopy studies

There is a significant presence of tiny spherical shaped TiO_2 nanoparticles in TEM photographs of the powders from 0.01M KOH and 0.1M KOH (6 hours and 12 hours) (Figure 2). This is consistent with XRD observations, indicating that higher [KOH] will provide higher driving force, hence a faster reaction rate. TEM observations also demonstrate that the initial [KOH] has stronger effect on the PbTiO_3 morphologies than the processing time. The change of [KOH] not only affected the reaction rate, but also altered the crystal growth mechanism and anisotropy. At 0.01M KOH, the crystal growth did not strongly depend on growth direction, resulting in irregular, rounded shaped morphology. The large particle size, slow consumption rate of TiO_2 and relatively narrower size distribution indicate that the nucleation rate in 0.01M KOH suspension was very low, and the reaction was dominated by coarsening of the particles. The mechanism might involve dissolution of TiO_2 and precipitation of PbTiO_3 on the particle surface. At [KOH] of 1.0M, the particle growth was highly anisotropic, resulting in rectangular shaped, (001) faceted, platelet morphology. At 0.1M KOH, TEM photographs revealed a "finger like" morphology, characterized by several columnar structures $\sim 25\text{nm}$ in width, $\sim 150\text{nm}$ in length, parallelly growing on a substrate. Strong evidence of secondary nucleation can be observed. The surface roughness change due to secondary nucleation might change the local reagent distribution, resulting in 1-D preferential crystal growth.

The influence of [KOH] on nucleation and grain growth was different. At low pH, the concentration of reagents could hardly initiate nuclei, resulting in a very low nucleation density. The transformation of feedstock to PbTiO_3 would be dominated by continuous coarsening of the existed particles. At high [KOH], the strong supersaturation could cause a homogeneous nucleation inside the suspension, majority of the feedstock would be consumed in this stage and therefore inhibit further nucleation. The higher solubility of PbTiO_3 at high

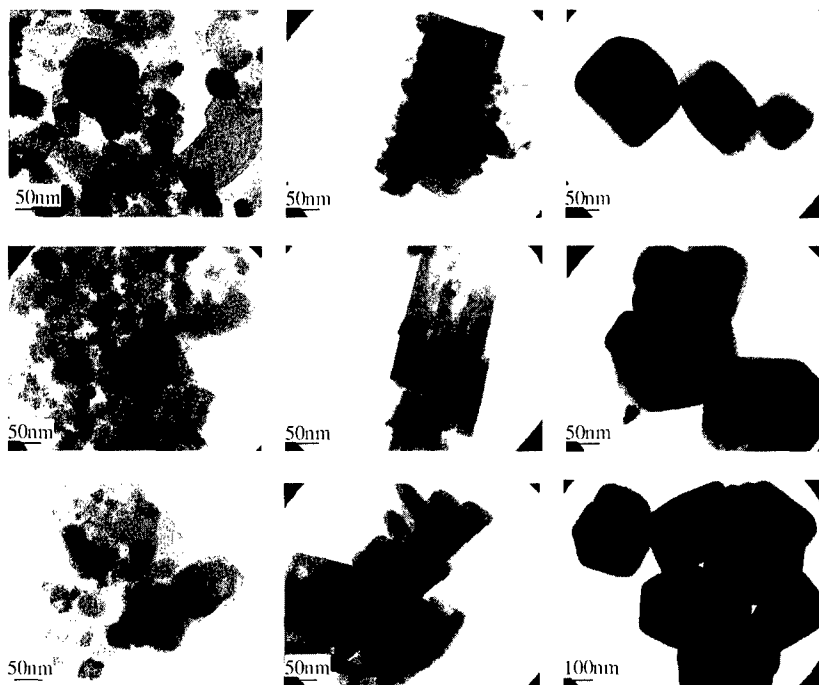


Figure 2. Morphology evolution as a function of processing time and initial KOH concentrations. From top to bottom, the processing time is 6 hours, 12 hours and 24 hours, respectively. From left to right, the initial [KOH] is 0.01M, 0.1M and 1.0M respectively. The spherical shaped particles with size $\sim 25\text{nm}$ are residual TiO_2 , which is the most visible in first column.

pH could effectively prompt the dissolution-precipitation process, which might dominate the coarsening in this case. At intermediate [KOH], nucleation and grain growth could occur spontaneously, resulting in a high possibility of secondary nucleation and a broader size distribution.

CONCLUSIONS

The initial concentration of KOH has strong influence on the morphology of hydrothermally derived PbTiO_3 nanoparticles. Low [KOH] revealed rounded particles while high [KOH] resulted in faceted platelet structure. Both low and high [KOH] give narrower size distribution than the intermediate [KOH]. Particles from intermediate [KOH] show a characteristic “finger like” morphology. The observations have been explained with a nucleation-growth competition mechanism.

ACKNOWLEDGMENTS

This work was partly supported by the National science Foundation grant # DMR 0096147. Z. Ye is grateful for support from the Purdue Electron Microscopy Consortium.

REFERENCES

1. W.J. Dawson, *Ceram. Bull.* **67**, 1673 (1988).
2. H. Cheng, J. Ma, Z. Zhao, and D. Qiang, *J. Am. Ceram. Soc.* **75**, 1123 (1992).
3. G.A. Rossetti Jr., D.J. Waston, R.E. Newnham, and J.H. Adair, *J. Crystal Growth* **116**, 251 (1992).
4. M.M. Lencka and R.E. Riman, *J. Am. Ceram. Soc.* **76**, 2649 (1993).
5. J.O. Eckert Jr., C.C. Hung-Huston, B.L. Gersten, M.M. Lencka, and R.E. Riman, *J. Am. Ceram. Soc.* **79**, 2929 (1996).
6. E.B. Slamovich and I.A. Aksay, *J. Am. Ceram. Soc.* **79**, 239 (1996).
7. A.T. Chien, J. Sachleben, J.H. Kim, J.S. Speak, and F.F. Lange, *J. Mater. Res.* **14**, 3303, (1999).
8. C.R. Peterson and E.B. Slamovich, *J. Am. Ceram. Soc.* **82**, 241 (1999).
9. C.R. Peterson and E.B. Slamovich, *J. Am. Ceram. Soc.* **82**, 1702 (1999).
10. M.C. Gelabert, B.L. Gersten, and R.E. Riman, *J. Crystal Growth* **211**, 497 (2000).
11. M.C. Gelabert, R.A. Laudise, R.E. Riman, *J. Crystal Growth* **197**, 195 (1999).
12. B. Jiang, J.L. Peng, L.A. Bursill and W.L. Zhong, *J. Appl. Phys.* **87**, 3462 (2000).
13. B. Jiang and L. A. Bursill, *Phys. Rev. B* **60**, 9978 (1999).